Electronic Supplementary Information

Flash-Joule Heating Enables Rapid Solid-State Synthesis of Multinary Chalcogenides: A Case Study on $Cu_2Mo_6S_8$

Pranay Ninawe,[a†] Cocoro A. Nagasaka,[a†] and Jesús M. Velázquez*[a]

[a] *Department of Chemistry, University of California, Davis, One Shields Avenue, Davis, California 95616, United States*

† Contributed Equally

**Corresponding author: email: jevelazquez@ucdavis.edu*

Table of Contents **Page**

Experimental Methods

Materials:

MoS_2 powder (>98%, ~325 mesh) and Graphite (20+100 mesh, 99% C) was purchased from Thermo Scientific, Mo powder (99.99%, ~250 mesh), FeS powder and Cu_2S powder (99.5%, ~200 mesh) were used as purchased from Sigma-Aldrich. S powder (99.5%) was purchased from Alfa Aesar. Fused silica tubes and Graphite plugs were purchased from ACS materials. Carbon Black (Vulcans XC-72R) was purchased from FuelCellStore.

Structural and spectroscopic characterization:

The reaction was carried out in an ACS Helio Volt Flash-Joule setup. Structural characterization and the phase purity of $Cu_2Mo_6S_8$ were carried out via PXRD measurements using a Bruker D8 Advance diffractometer with Cu K-alpha radiation (1.54 Å). The FEI Scios Dual Beam FIB/ scanning electron microscope (SEM) system was used to probe the morphology. An Oxford energy-dispersive X-ray (EDX) detector was used to confirm the stoichiometry and the uniform distribution of all the elements across the samples. Surface composition was probed *via* X-ray photoelectron spectroscopy (XPS) using a Kratos Supra Axis spectrometer with an Al anode (1486.6 eV).

X-ray absorption spectroscopy (XAS) measurements were performed at the Stanford Synchrotron Radiation Lightsource, located at the SLAC National Accelerator Laboratory. X-ray Absorption Near-Edge Structure (XANES) spectra at the S K-edge, Cu K-edge, and Mo L_3-edge were collected at beamline 4-3. The incident beam energy was calibrated using sodium thiosulfate as a standard for the S K-edge, while a copper metal foil served as the reference for Cu calibration. Tender X-ray measurements were conducted under a He atmosphere to minimize fluorescence signal attenuation caused by air absorption at lower energies. For each material, three fluorescence scans were acquired using a Lytle detector to ensure reproducibility and signal quality.

Figures & Tables

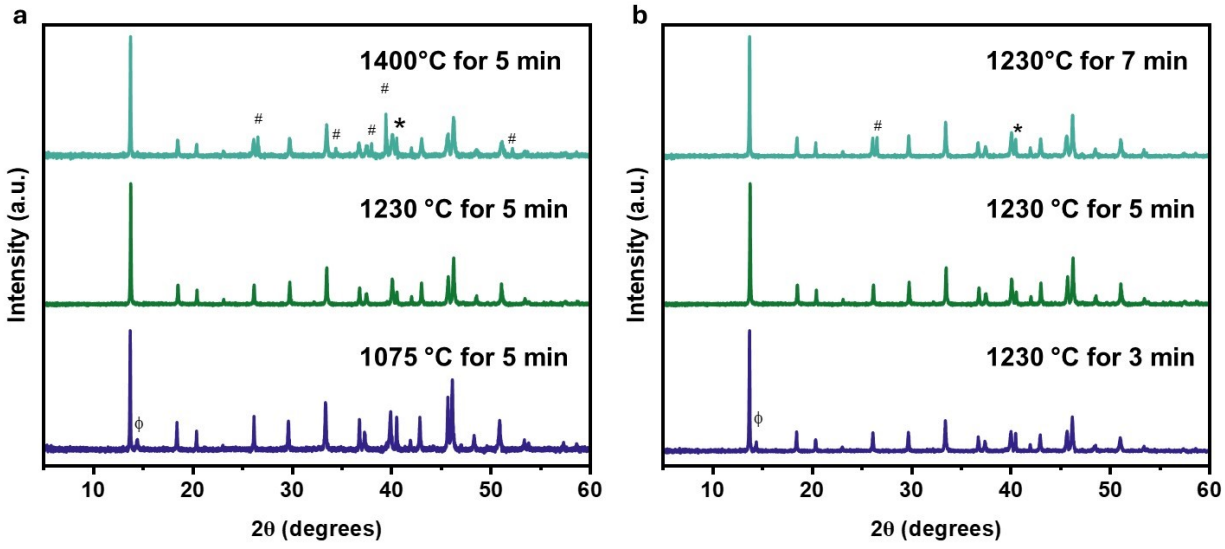

Figure S1. Powder X-ray Diffraction Pattern as a function of (a) Temperature and (b) Time in the step-heating mode. (the symbols represent the impurities, ϕ - MoS_2, ∗ - Mo, # - Mo oxides)

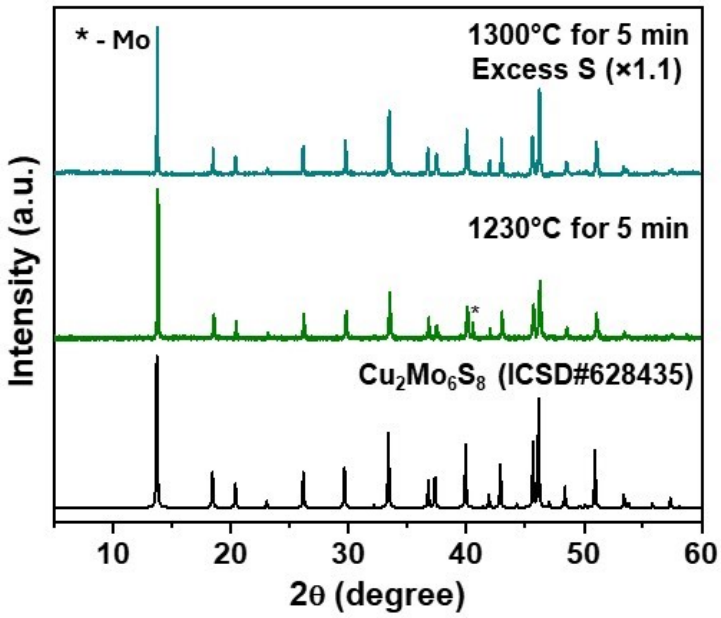

Figure S2. Powder X-ray Diffraction Pattern of $Cu_2Mo_6S_8$ synthesized using the optimized reaction conditions for step-heating mode. (The symbol (*) represent the Mo impurity)

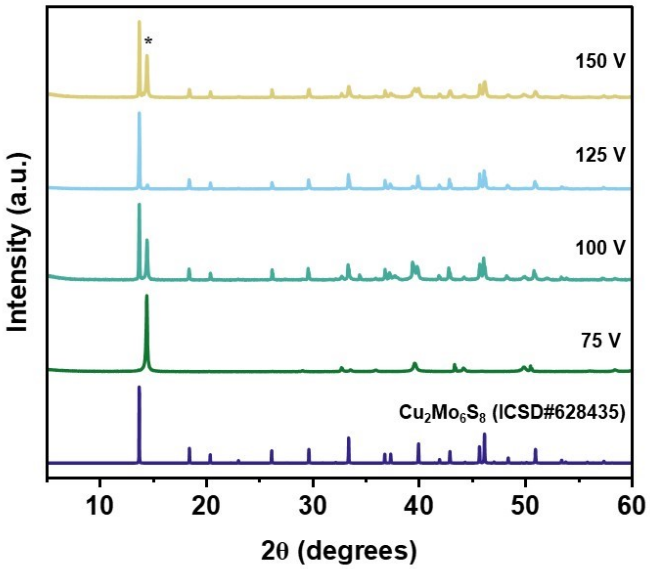

Figure S3. Powder X-ray Diffraction Pattern of $Cu_2Mo_6S_8$ as a function of applied voltage in the flash-heating mode. (The symbol (*) represent the MoS_2 impurity)

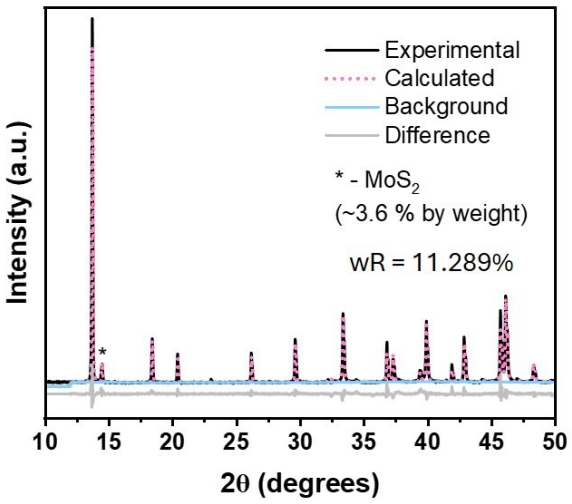

Figure S4. Rietveld refinement of powder X-ray diffraction pattern of $Cu_2Mo_6S_8$ synthesized in the flash-heating mode at 125 V.

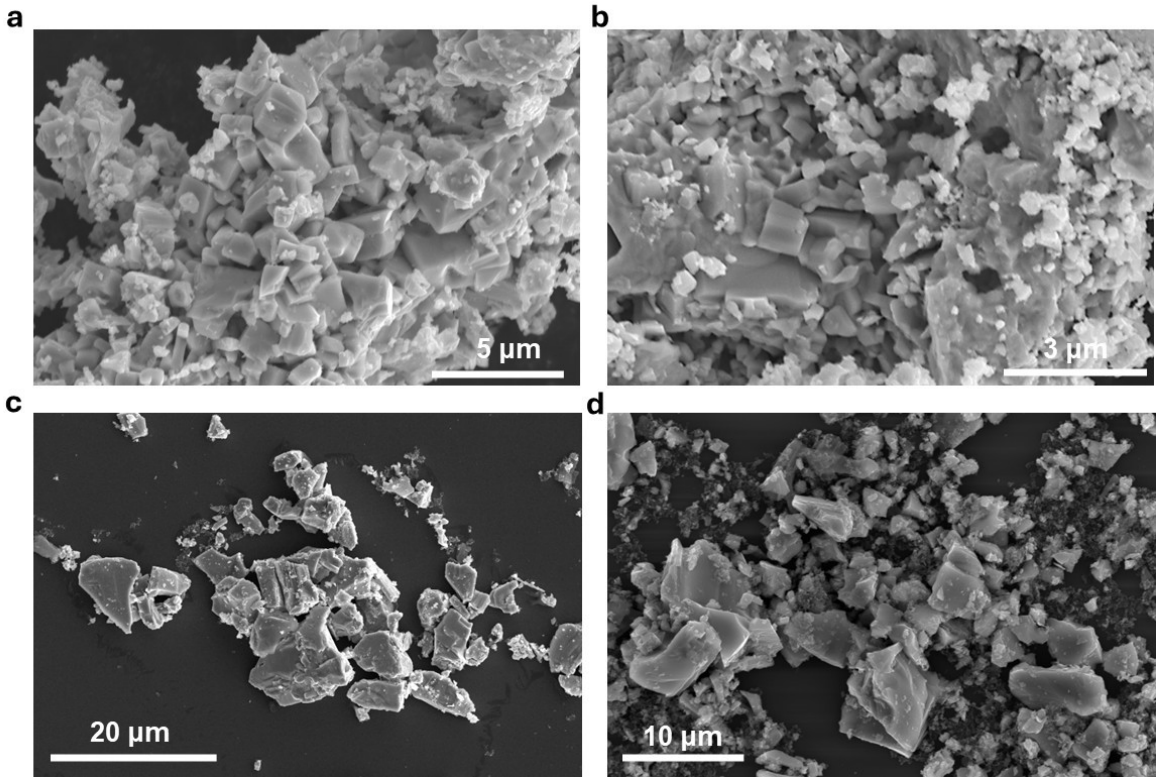

Figure S5. Scanning electron microscopy (SEM) images of $Cu_2Mo_6S_8$ synthesized using (a-b) step -heating and (c-d) flash-heating.

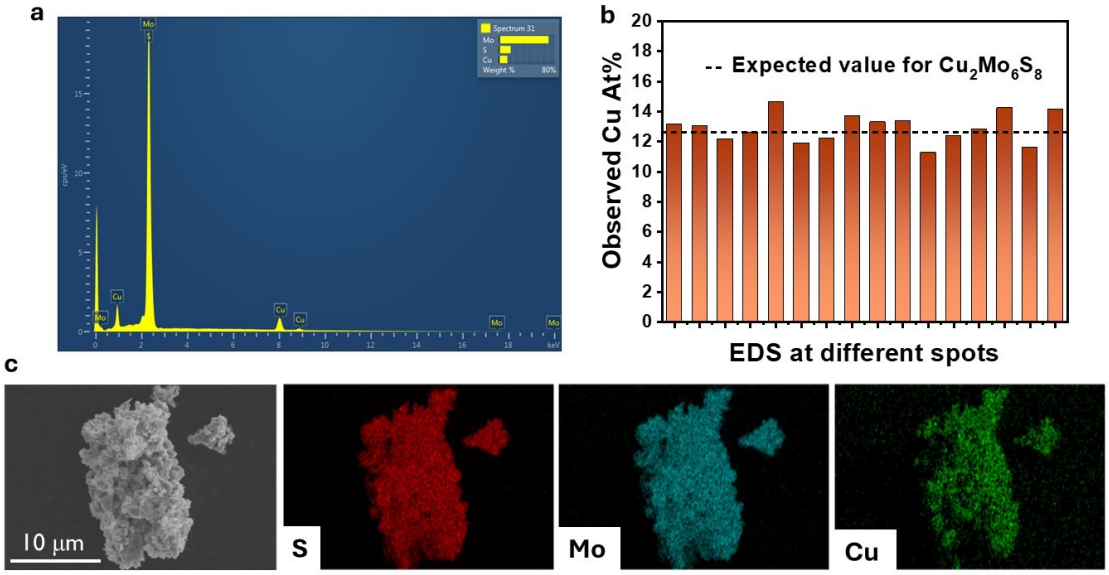

Figure S6. Energy dispersive X-ray spectroscopy (EDS): (a) spectra, (b) observed Cu At % at different spots, (c) mapping of $Cu_2Mo_6S_8$ synthesized using step-heating mode.

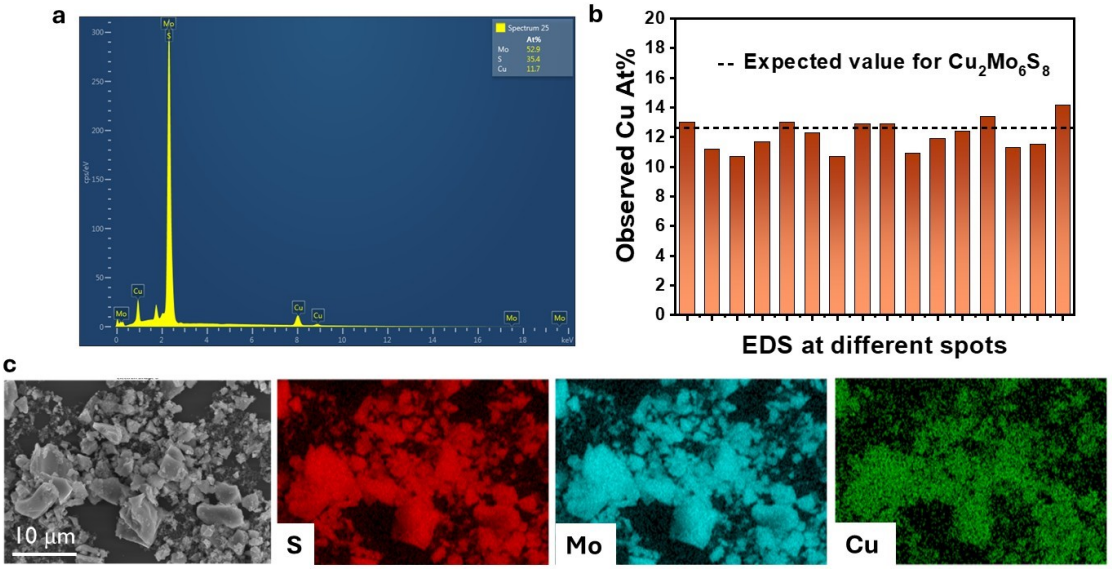

Figure S7. Energy dispersive X-ray spectroscopy (EDS): (a) spectra, (b) observed Cu At % at different spots, (c) mapping of $Cu_2Mo_6S_8$ synthesized using flash-heating mode.

Table S1: Flash and Step heating comparison for $Cu_2Mo_6S_8$

Heating Mode	Step Heating	Flash heating
Heating mechanism	Resistive heating	Capacitive discharge
Heating rate	Slow - Continuous heating	Fast - Pulse heating
Use case	Scalable bulk synthesis	Accessing metastable phases
Reaction Time	5 minutes	1-2 s
Reaction Temperature	~1300 °C	~2000 °C
Impurities	None	MoS_2
Morphology	Cuboidal crystallites	Irregular

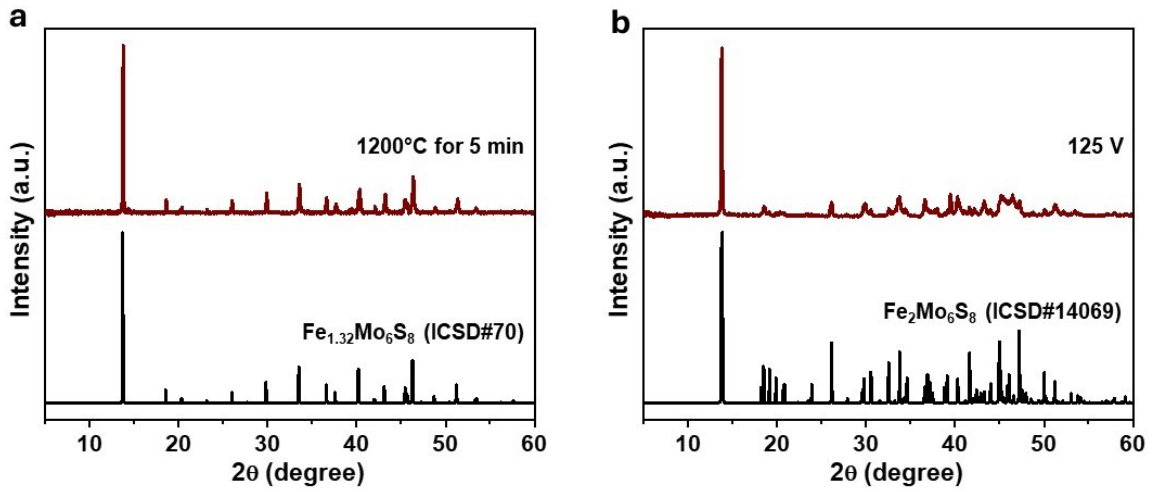

Figure S8. Powder X-ray Diffraction Pattern of (a) $Fe_{1.32}Mo_6S_8$ synthesized using the step-heating mode and (b) $Fe_2Mo_6S_8$ synthesized using the flash-heating mode.

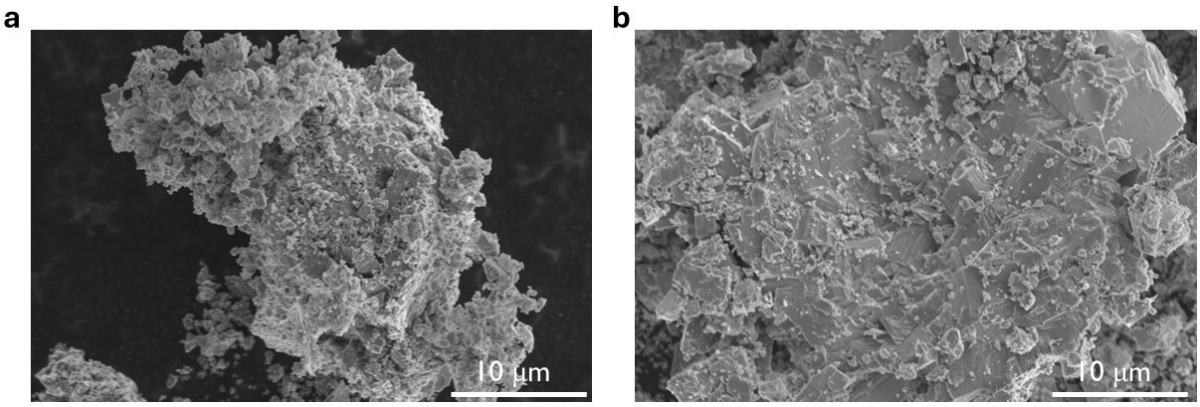

Figure S9. Scanning electron microscopy (SEM) images of (a) $Fe_{1.32}Mo_6S_8$ synthesized using the step heating mode and (b) $Fe_2Mo_6S_8$ synthesized using the flash heating mode.

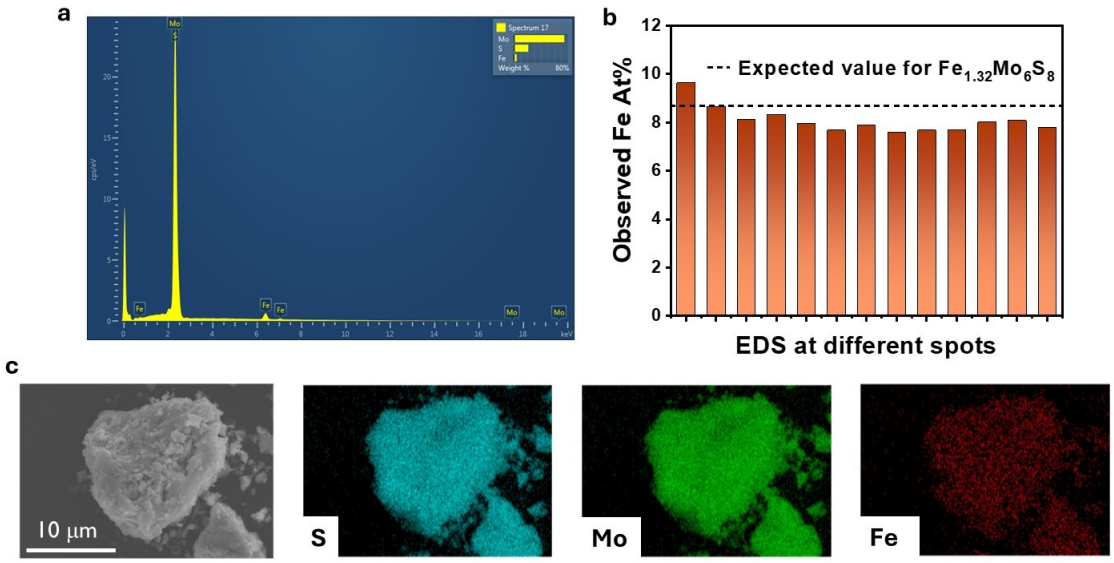

Figure S10. Energy dispersive x-ray spectroscopy (EDS): (a) spectra, (b) observed Fe At % at different spots, (c) mapping of $Fe_{1.32}Mo_6S_8$ synthesized using step-heating mode.

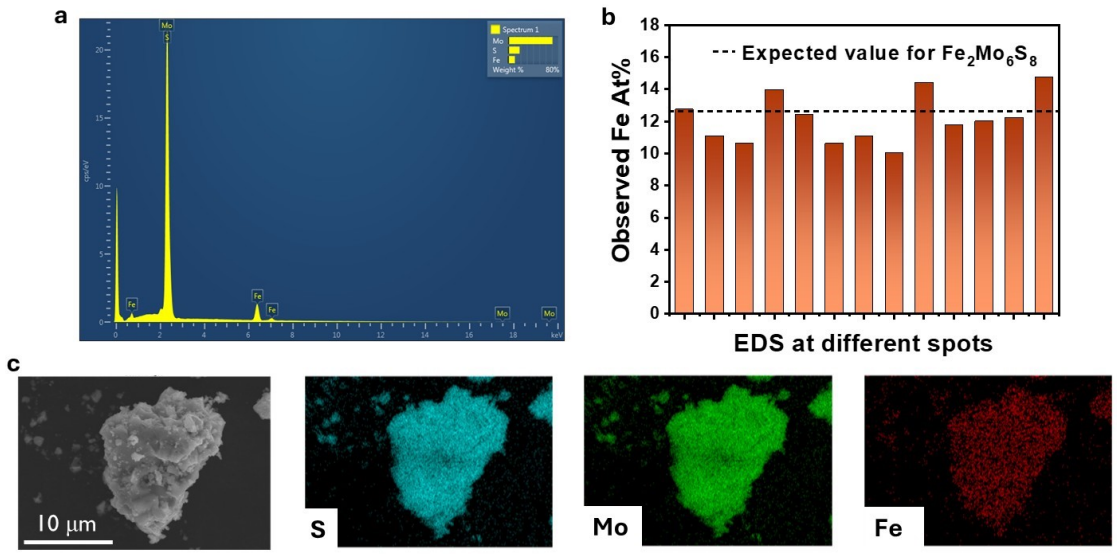

Figure S11. Energy dispersive x-ray spectroscopy (EDS): (a) spectra, (b) observed Fe At % at different spots, (c) mapping of $Fe_2Mo_6S_8$ synthesized using flash-heating mode.

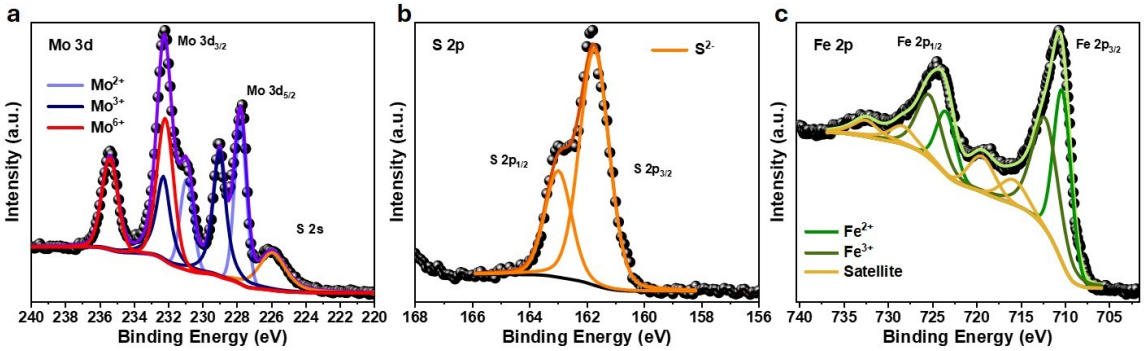

Figure S12. High-resolution X-ray photoelectron spectroscopy (XPS) spectra of (a) Mo 3d (b) S 2p and (c) Fe 2p for $Fe_{1.32}Mo_6S_8$.

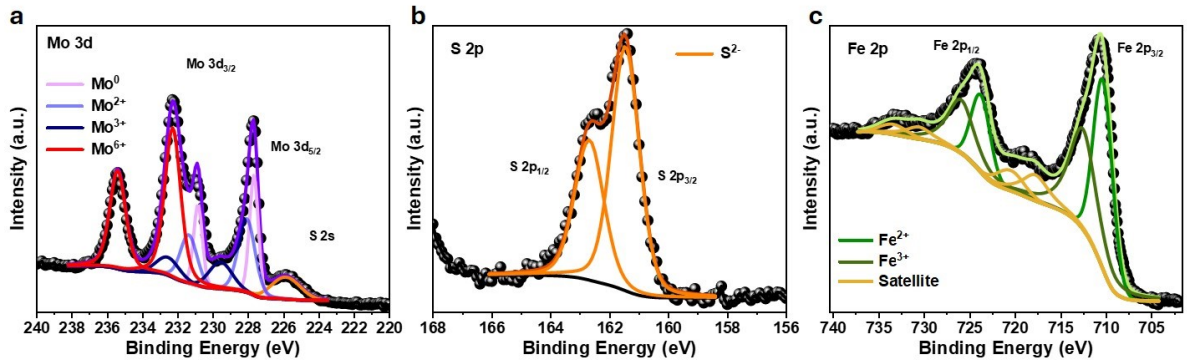

Figure S13. High-resolution X-ray photoelectron spectroscopy (XPS) spectra of (a) Mo 3d (b) S 2p and (c) Fe 2p for $Fe_2Mo_6S_8$.

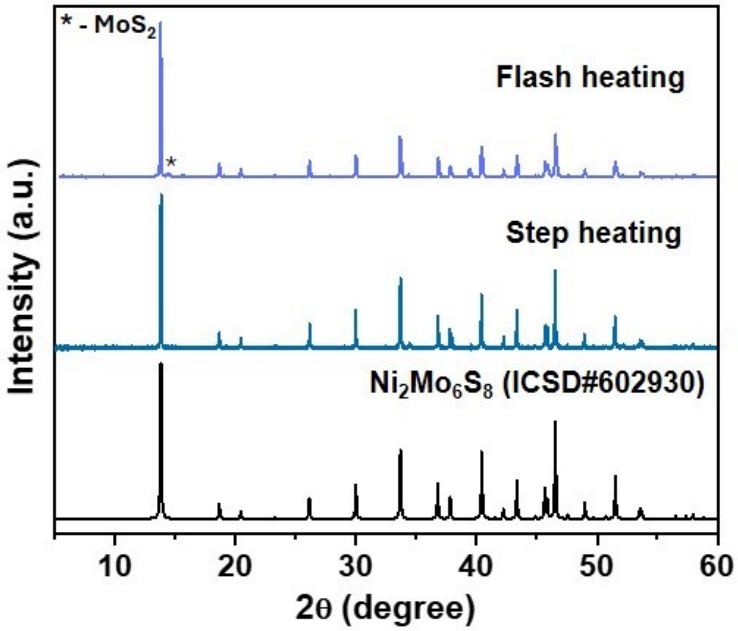

Figure S14. Powder X-ray Diffraction Pattern of $Ni_2Mo_6S_8$ synthesized using the step-heating mode and flash-heating mode.

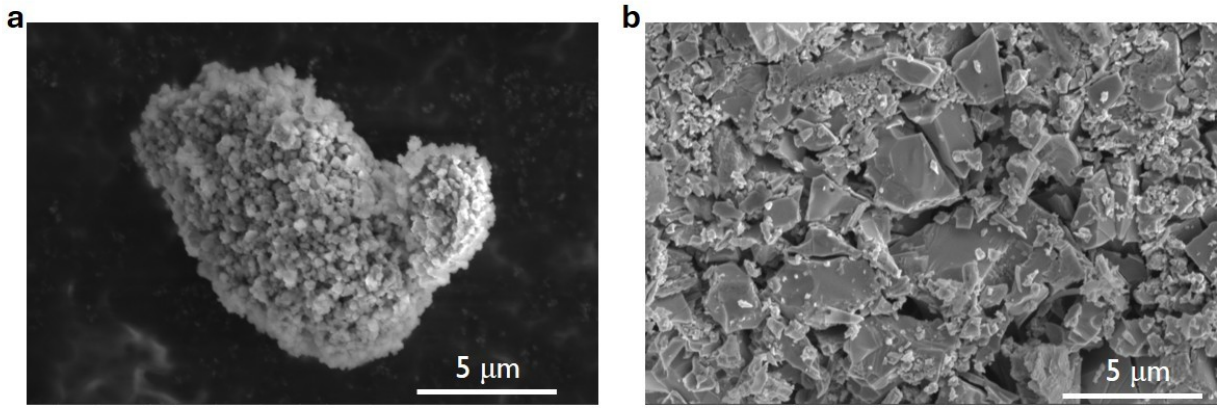

Figure S15. Scanning electron microscopy (SEM) images of $Ni_2Mo_6S_8$ synthesized using the (a) flash heating mode and (b) step heating mode.

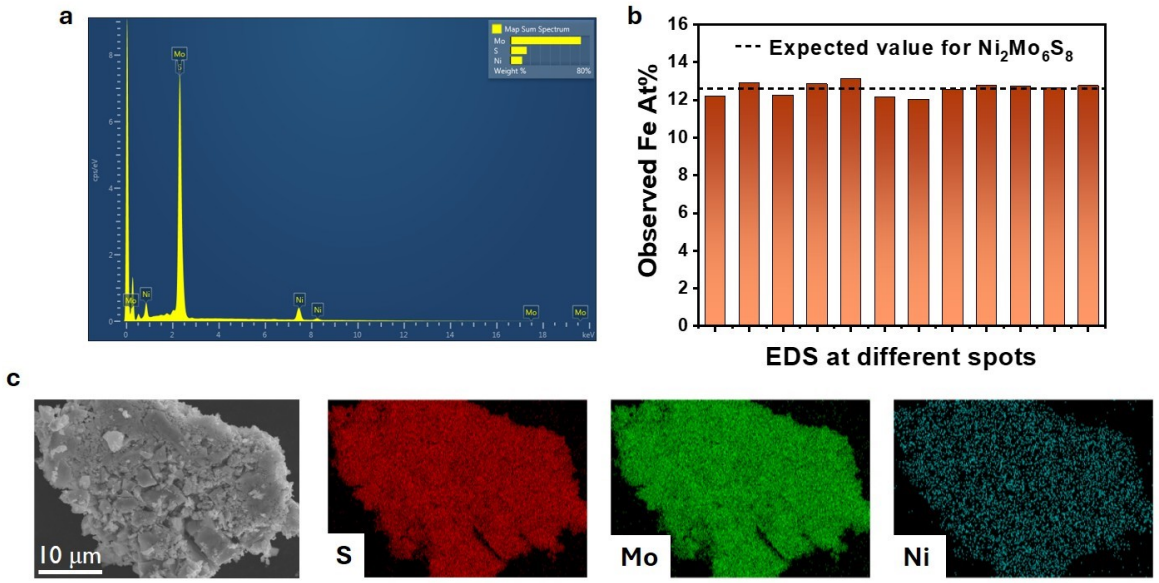

Figure S16. Energy dispersive x-ray spectroscopy (EDS): (a) spectra, (b) observed Ni At % at different spots, (c) mapping of $Ni_2Mo_6S_8$ synthesized using step-heating mode.

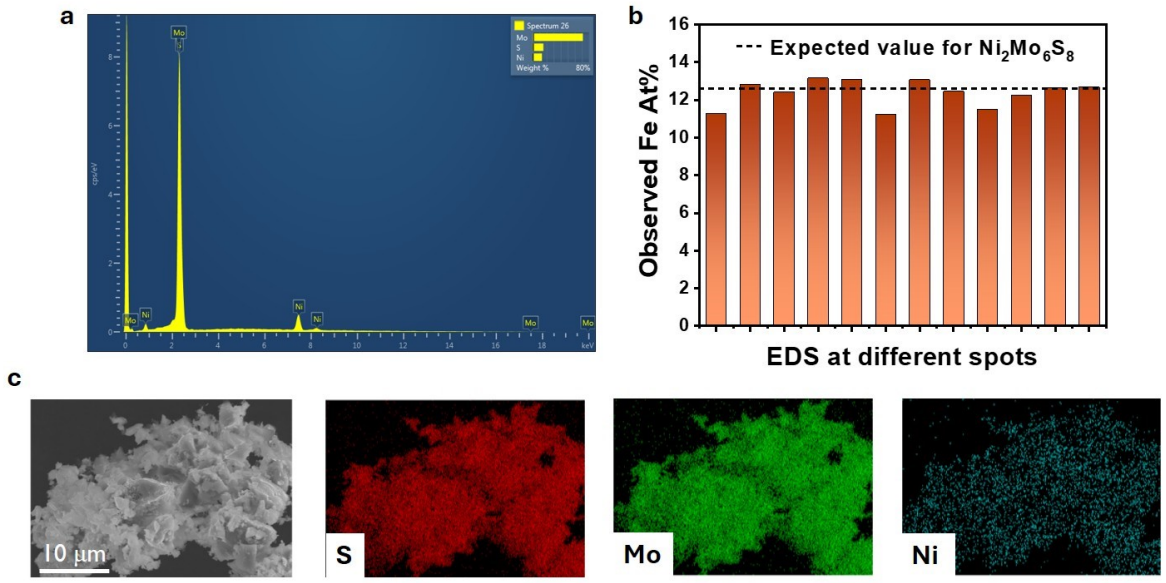

Figure S17. Energy dispersive x-ray spectroscopy (EDS): (a) spectra, (b) observed Ni At % at different spots, (c) mapping of $Ni_2Mo_6S_8$ synthesized using flash-heating mode.

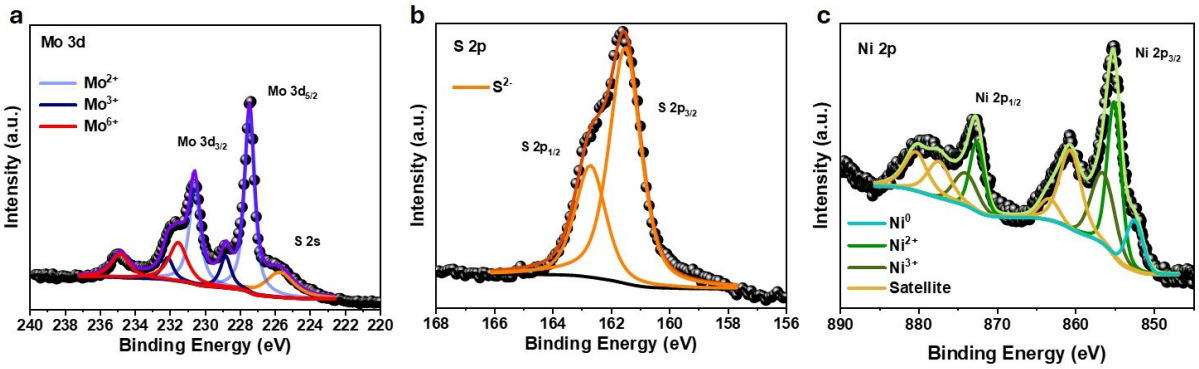

Figure S18. High-resolution X-ray photoelectron spectroscopy (XPS) spectra of (a) Mo 3d (b) S 2p and (c) Ni 2p for $Fe_2Mo_6S_8$ synthesized using Step mode.

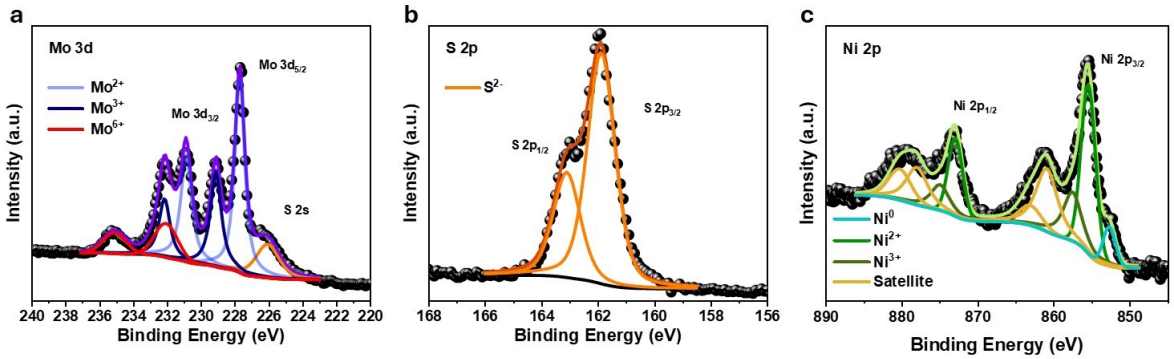

Figure S19. High-resolution X-ray photoelectron spectroscopy (XPS) spectra of (a) Mo 3d (b) S 2p and (c) Ni 2p for $Fe_2Mo_6S_8$ synthesized using Flash mode.

Table S2: Estimation of Energy Consumption for $Cu_2Mo_6S_8$ Synthesis Using Flash, Step, Microwave, and Conventional Furnace Heating Methods

Heating Mode	Furnace	Microwave	Step Heating	Flash heating
Heating mechanism	External resistive heating	Dielectric/Microwave absorption	Joule heating	Capacitive discharge
Heating rate	Slow - Continuous heating (5-20 °C min^{-1})	Fast - Continuous heating (~40 °C s^{-1})	Fast - Continuous heating (~50 °C s^{-1})	Extremely rapid - Pulse heating (10^3–10^5 °C s^{-1})
Reaction Time	~24 hours	~10 minutes	~5 minutes	< 1 s
Reaction Temperature	~1100 °C	~1100 - 1200 °C	~1300 °C	~2000 °C
Power	1.5 kW	1.2 kW	-	-
Energy Equation (E)	Power rating × t (s)	Power × t (s)	V × I × t	½ C × V^2
Approximate Energy required (kWh)	~36	~0.2	~0.01	~10^{-4}
Reference	Y-J Kim., et.al. *RSC Adv.*, **2014**, *4*, 59048-59055	J. M. Velazquez., *J. Coord. Chem*. **2019**, *72*, 1322–1335.	This work	This work

t = time; R = Resistance (ohm); I = Current (A); V = Voltage (V); C = Capacitance (F)